Proceedings of the 2023 Winter Simulation Conference
C. G. Corlu, S. R. Hunter, H. Lam, B. S. Onggo, J. Shortle, and B. Biller, eds.

A COMPARISON OF LISSAJOUS CURVES TO TRADITIONAL PATTERNS IN AERIAL SEARCH SIMULATIONS

Mitchell J. Miller
Victor E. Trujillo
James E. Bluman

Department of Mathematical Sciences
United States Military Academy
606 Thayer Road
West Point, NY 10996, USA

J. Josiah Steckenrider

Department of Civil and Mechanical Engineering
United States Military Academy
606 Thayer Road
West Point, NY 10996, USA

ABSTRACT

Technological advancements have made autonomous aerial search using unmanned systems a promising approach to search and rescue, targeting, and other mission sets. A handful of standard flight paths are traditionally used for aerial search, but this research presents the Lissajous pattern as an alternative to these traditional paths that could potentially locate targets more quickly. This research considers a searching agent with imperfect detection capability and leverages Monte Carlo simulations to generate data for various flight paths. Each flight path is evaluated by cumulative density functions representing the time it takes an unmanned aircraft system (UAS) to reach some desired percent certainty of locating a randomly generated target in a search area. Results show that Lissajous curves are viable search paths for superior aerial target detection, particularly for evasive targets in a Reciprocal Gaussian sampling distribution.

1 INTRODUCTION

1.1 Purpose and Motivation

Unmanned aircraft systems (UASs) are becoming increasingly prevalent throughout the world, and their civilian and military applications are rapidly expanding. Many tasks and activities are more safely and efficiently accomplished from the air by autonomous agents than manually by human workers. Some significant civilian applications include search and rescue (SAR) missions (Mishra et al. 2020), fertilizer spreading in agriculture (Dutta and Goswami 2020), and even geoscientific analysis through aerial imaging (Niedzielski 2018). On the military side, combat search and rescue (CSAR) is an important application (Ayers and Wahlman 2021), as are other intelligence, surveillance, and reconnaissance (ISR) missions (Paucar 2018). In many of these applications, pre-determined flight paths are often used to quickly and comprehensively cover a region of interest. Though flight paths can be used to accomplish a number of tasks, this paper specifically deals with the problem of generalized aerial search.

To motivate the need for robust autonomous aerial search, one may consider the application of maritime search and rescue, which lies at the intersection of civilian and military interests. The U.S. Coast Guard first established its UAS Program Office in 2008 (United States Coast Guard Aviation History 2008). The Coast Guard averaged 323 lives lost per year in SAR missions prior to 2008, but since establishing this program, the number has dropped to only 182 (Bureau of Transportation Statistics 2017). This demonstrates that deployment of UASs can improve the success rate of search missions, but refining UAS search paths could yield even further improvement. The research presented here examines the efficacy of UAS search patterns based on Lissajous curves for finding targets using a rectangular projected field-of-view (FOV).

Building on previous work (Blankenship et al. 2021), this research develops a framework to validate and optimize Lissajous search patterns for different scenarios given mission variables such as target behavior (initial belief distribution), acceptable risk level (certainty threshold), payload capabilities such as camera quality (time constant), and FOV size.

1.2 Background

This research implements deterministic path planning for aerial search. A deterministic flight path means that the entire route is pre-planned before the search agent is ever deployed. In contrast, information-theoretic approaches use online information acquired during search to continuously change the path. Information-theoretic approaches have an intuitive edge owing to their adaptive nature; however, they come with a higher computational expense and are ineffective when information about the target or the environment is unavailable (Steckenrider et al. 2020). Herein lies the motivation for pursuing a deterministic solution for pre-mission path design. Another benefit of deterministic path planning is that such patterns can be used in manned missions and not solely autonomous ones.

The International Aeronautical and Maritime Search and Rescue (IAMSAR) Manual presents the "expanding square" and "parallel track" patterns as two of the standard deterministic flight patterns used in SAR missions (IMO 2016). These flight paths are also referred to as the "expanding spiral" (ES) and "horizontal sweep" (HS) respectively, and are shown in Figure 1 (Blankenship et al. 2022). Another standard deterministic flight pattern worthy of mention is the triangular sector search. While not explored in this analysis, it is a viable pattern that future research could examine. These patterns are attractive for automated search because they are guaranteed to cover an entire search area over a long enough period of time. However, this potentially large time cost raises some concerns. If the target resides along the outside of the search area (in relation to the expanding spiral) or on the opposite side of the search area (in relation to the horizontal sweep), then the UAS will not locate it quickly. While the guarantee of 100% area coverage is a favorable property, many search missions also value timeliness in finding targets. This is why we favor the alternative option of the Lissajous pattern to these canonically employed deterministic flight paths.

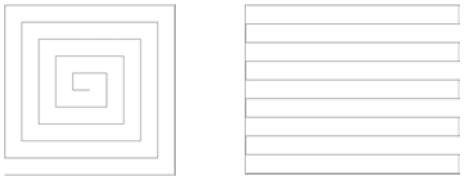

Figure 1: Expanding spiral and horizontal sweep Search Patterns.

The Lissajous pattern (Figure 2), is a deterministic path that can balance comprehensiveness with speed (Blankenship et al. 2021). With open space between its large, sweeping movements through the middle of a search area, the Lissajous is not guaranteed to achieve 100% coverage. However, it does travel through each subdomain of the search area faster than the standard patterns take to traverse its entirety. By sacrificing a small level of certainty in locating a target, a Lissajous pattern may still locate targets a majority of the time much faster than traditional patterns.

Mathematically, a Lissajous curve is a set of parametric equations based on harmonic motion as depicted in Equations (1),

$$x(t) = A_x \sin(\omega_x t + \varphi_x) \tag{1a}$$

$$y(t) = A_y \sin(\omega_y t + \varphi_y), \tag{1b}$$

where A is amplitude, ω is frequency, and φ is phase shift. The pattern is attractive as a search path given its adaptability via the ratio of frequencies $r_\omega = \frac{\omega_x}{\omega_y}$. Through small changes in this frequency ratio, an

infinite number of different patterns can be generated, from lines to circles to figure-8's (Blankenship et al. 2021). Patterns with irrational frequency ratios will never repeat and will therefore eventually cover an entire search domain.

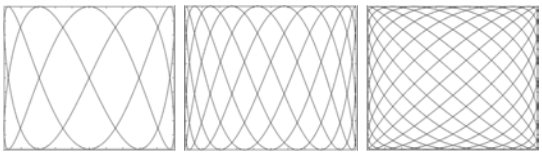

Figure 2: Example Lissajous patterns.

1.3 Research Objectives

One primary objective of this research is to investigate the conditions under which Lissajous patterns outperform traditional deterministic patterns, specifically when a small target is sought with an optical sensor with a rectangular FOV. This leads to the nontrivial determination of a suitable metric for probabilistically evaluating the performance of a search pattern. Another important objective is to determine which frequency ratios perform best for a given search scenario. Finally, the influence of an aerial sensor's probability of detection (POD) on the optimality of a Lissajous pattern is investigated. These objectives are pursued by conducting Monte Carlo simulation experiments and extracting conclusions from statistical results.

In order to address the above, several assumptions that frame the Monte Carlo simulations must be described. First, we assume that the aerial search problem is effectively two dimensional. The ground image that the search agent sees with a downward-facing camera is modeled by a rectangular FOV sweeping across the search space, whose relative size is dictated by the agent's altitude. This is addressed in part by generating simulations with varying UAS FOV sizes. We also neglect flight physics and any motion of targets in the search space when conducting Monte Carlo experiments. These are all elements which we plan to address in future iterations of this research.

2 METHODOLOGY

2.1 Monte Carlo Simulation

Due to the intractability of analytically optimizing Lissajous curves, a Monte Carlo simulation approach was taken to generate data for evaluating search paths in this research. As depicted in the left part of Figure 3, the simulation randomly generates a target in a one-by-one unit search space. We keep all dimensions, other than time, unitless to preserve broad applicability. A UAS with a set FOV size then travels through the search area on a particular flight path–either a Lissajous pattern with a set frequency ratio, an expanding spiral, or a horizontal sweep. When the FOV passes over the target, it is probabilistically "detected" (see Sec. 2.3).

The simulation randomly generates k targets in the search space as shown in Figure 3. Sending the search agent over the prescribed path and recording the time at which each target is located generates a cumulative density function (CDF). These CDFs give the probability that any single randomly located target was detected before the corresponding time (seconds) by a UAS with a selected flight path. Each point along the CDF represents a single target and the time taken to locate it. (See Sec. 3 for visual examples of CDF outputs from the simulations.)

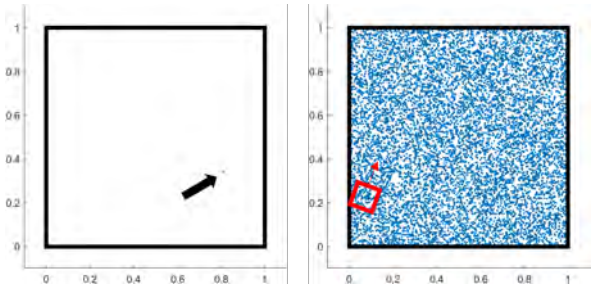

Figure 3: Simulation showing a single generated target (left) and $k = 10000$ uniformly generated targets (right). The red square represents the agent's FOV (1% of the overall search area).

2.2 Convergence Study

Given the use of simulation-based methods, each search path must be executed enough times to yield consistent data. A convergence study revealed that $k = 10,000$ iterations of the simulation (i.e. 10,000 targets generated in the search area) for a given flight path was adequate to attain these consistent results. Naturally, the more iterations performed, the more consistent and repeatable the results will be. However, the simulation trades computational efficiency for each iteration it performs. To determine the adequacy of 10,000 iterations, a search scenario was simulated 500 times, each with a different number of iterations between 1 and 100,000. Each simulation produced a CDF, with the simulation of 100,000 iterations being considered the "ground-truth" CDF. The CDF accuracy only marginally improves between 10,000 and 20,000 iterations, with the RMSE changing by only 0.00055. This justifies 10,000 iterations as a reasonable number for this research.

2.3 Probabilistic Target Detection

In order to broadly capture the behavior of an aerial field detector without the computational burden of low-level vision simulation, a probabilistic model for target detection is employed. Because missed detections will undoubtedly occur in autonomous (or even manned) visual search, the probability of target detection is broadly modeled as a function of the amount of time that a given target is inside an agent's FOV. As adapted from Stone (1975), this probability of detection is given by:

$$p(t_d) = 1 - \exp\left(\frac{t_d}{\tau}\right), \tag{2}$$

for $t_d \geq 0$, where t_d is the *detectable time*, defined as the amount of time in seconds that a target was within the FOV of a search agent. This POD model maps a target's detectable time to its probability of having been detected, as influenced by the time constant parameter τ. Section 2.6.4 provides a more detailed exploration of the time constant. This parameter effectively models the quality of a given detector.

Determining the detectable time for a target requires counting the time steps during which the target is within a searcher's FOV. This becomes a geometric problem which asks, "Given a target's location $\mathbf{x}_T = [x_T \quad y_T]^\top$ in 2D space, determine if that point falls within the boundaries of a rectangle of width w and height h, centered at coordinates $\mathbf{x}_A = [x_A \quad y_A]^\top$, oriented at an angle θ." Since this problem must be solved for all 10,000 targets in any given simulation, it is important to solve with computational efficiency in mind. As such, the following initial qualifying filter is applied to all targets:

$$||\mathbf{x}_{T_i} - \mathbf{x}_A||_2 < \sqrt{(h/2)^2 + (w/2)^2}.$$

If this condition is true for the i^{th} target, it is further considered for detection. If not, no additional checks are implemented since the target and agent are too far from one another (in a 2D sense) for the target to possibly fall within the FOV.

The second and final check of whether or not a target has been detected solves the geometric problem stated above. Since the FOV may be oriented at any angle θ in the plane, it is difficult to directly assess whether a target is located within the FOV. For this reason, a coordinate system transformation is first implemented which greatly simplifies this task. The i^{th} target's location is transformed into the frame of the search agent by

$$\mathbf{x}'_{T_i} = \mathbf{R}(-\theta)(\mathbf{x}_{T_i} - \mathbf{x}_A),$$

where $\mathbf{R}(-\theta)$ is a 2D rotation matrix. Finally, a target is determined to have been detected if the following conditions are true:

$$-w/2 < x'_{T_i} < w/2, \quad -h/2 < y'_{T_i} < h/2.$$

If this is satisfied for a particular target, the number of time steps used to compute the detectable time for that target is incremented.

2.4 Average Speed

Simulated search agents move along predetermined waypoints that trace out flight paths in a search area. In order to ensure fairness in the comparison between Lissajous patterns and traditional ES and HS patterns, search agents using any path must travel at the same average speed for the duration of each simulation. Because the standard deterministic patterns follow rectilinear paths, determining the waypoint spacing for a desired constant velocity is simple. However, Lissajous path waypoints are not constantly spaced: they become closer together around tight turns and more widely spaced across quasi-straight stretches, which means a Lissajous search agent will not move at a constant speed. Nonetheless, the average speed of the Lissajous pattern must still equal the speed of the other patterns to ensure a fair comparison.

The position of a search agent at some point in time along a Lissajous path is given by Equations (1). Therefore, the velocities of the agent are given by:

$$x'(t) = A_x \cos(\omega_x t + \varphi_x)\omega_x,$$
$$y'(t) = A_y \cos(\omega_y t + \varphi_y)\omega_y,$$

which implies that the speed of the agent is

$$s(t) = \sqrt{{A_x}^2 \cos^2(\omega_x t + \varphi_x){\omega_x}^2 + {A_y}^2 \cos^2(\omega_y t + \varphi_y){\omega_y}^2}.$$

The average speed over some time period T then becomes:

$$\bar{s}(T) = \frac{1}{T}\int_0^T s(t)\,dt = \frac{1}{T}\int_0^T \sqrt{{A_x}^2 \cos^2(\omega_x t + \varphi_x){\omega_x}^2 + {A_y}^2 \cos^2(\omega_y t + \varphi_y){\omega_y}^2}\,dt.$$

To simplify the problem, several parameters can be assumed without loss of generality in the problem space of this research. Assuming the searcher begins in the lower-right corner of the search domain, $\varphi_x = \frac{\pi}{2}$ and $\varphi_y = -\frac{\pi}{2}$. Since the efficacy of a Lissajous search pattern is independent of the size of the search space, it can further be assumed that $A_x = A_y = 1$. This simplifies Eq. 2.4 to:

$$\bar{s}(T) = \frac{1}{T}\int_0^T \sqrt{\sin^2(\omega_x t){\omega_x}^2 + \sin^2(\omega_y t){\omega_y}^2}\,dt.$$

Expressing this in terms of the frequency ratio $r_\omega = \frac{\omega_x}{\omega_y}$ gives:

$$\begin{aligned}\bar{s}(T) &= \frac{1}{T}\int_0^T \sqrt{\sin^2(\omega_x t){\omega_x}^2 + \sin^2\left(\frac{\omega_x}{r_\omega}t\right)\frac{\omega_x^2}{r_\omega^2}}\,dt \\ &= \frac{\omega_x}{T}\int_0^T \sqrt{\sin^2(\omega_x t) + \frac{1}{r_\omega^2}\sin^2\left(\frac{\omega_x}{r_\omega}t\right)}\,dt \end{aligned} \tag{4}$$

Even in this fully simplified form, Equation (4) is intractable and there is no closed-form analytic solution. To circumvent this issue, the average speeds of thousands of Lissajous patterns with different ω_x and r_ω values were generated and stored in a lookup table which is then referenced during simulations to obtain the required ω_x for a desired $\bar{s}(T)$. This approach ensures agreement of all patterns' average speeds with precision on the order of ten-thousandths, without the need for a closed-form solution for the Lissajous pattern's average speed.

2.5 Evaluation Metric

The simulation's output CDF provides holistic information about search pattern performance over time, but it does not provide a single summarizing value with which to compare patterns. Favoring the pattern that most quickly locates all k targets ignores the speed-certainty trade off of the Lissajous pattern. Instead, one could choose a certainty cutoff and test which search pattern can reach 85% certainty (for example) the fastest, but even this approach presents issues. A CDF could be underperforming over the entire simulation but then improve at just the right time to be considered the fastest to reach a desired certainty threshold. To resolve this issue, we propose the expected value from the CDF as the evaluation metric for comparing search patterns.

Visually, the expected value is the area above the CDF (Feller 1971), given mathematically as:

$$E(X) = \int_0^\infty (1 - F_X(x))\, dx,$$

where a lower expected value implies better search performance. This metric can be interpreted as the expected time at which a search mission is considered complete. The calculation is still paired with a certainty threshold, as to not ignore the Lissajous pattern's speed/certainty trade-off, where the upper bound of the integral is modified to be the time at which the CDF reaches said threshold. This provides a single summarizing value for pattern comparison which also has an intuitive interpretation from the CDF.

2.6 Simulation Parameters

Since Monte Carlo methods are used in this work to extract performance metrics from thousands of search scenario simulations, these scenario outcomes are highly dependent on several simulation parameters. Each of the critical parameters is detailed in a subsection below.

2.6.1 Frequency Ratio

Because the frequency ratio r_ω controls the "order", or basic shape, of a Lissajous curve, it is one of the most important parameters in this research. Determining whether a Lissajous search path is better than a traditional search path necessarily raises an intermediate question of which specific Lissajous patterns should be considered. Naturally, some Lissajous paths will perform considerably better than others given the infinite variability in shape based on frequency ratio. Figure 4 shows the relationship between the average time step at which a target is found and the frequency ratio used for the search pattern, with all other simulation parameters held constant. As the plot shows, frequency ratios around highly rational numbers (e.g. 1/2, 2/3, 4/5, etc.) demonstrate poor performance since those patterns very nearly repeat after a short time, leaving large unsearched gaps. (It is important to note that only frequency ratios in the range $(0, 1)$ were used since the simulated search space has 90° rotational symmetry.)

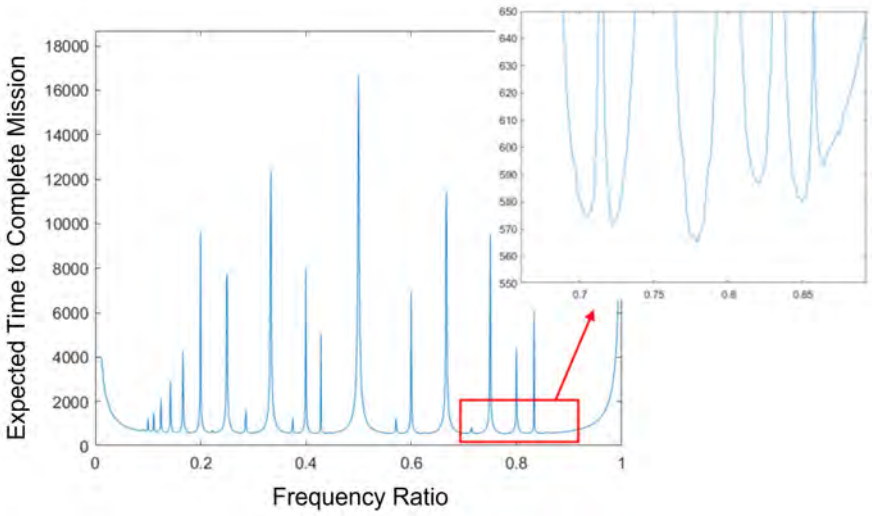

Figure 4: Expected mission completion time by Lissajous curve shape for optimizing frequency ratio given a set of simulation parameters.

2.6.2 Field of View Size

The FOV parameter adds an element of realism to the simulations, allowing different flight altitudes and sensor types to be broadly modeled. The FOV is modeled as a square, centered on the search agent's position at every time step, whose orientation remains perpendicular to the path of the searcher. In order to keep simulations dimensionless, the FOV size is specified as a percent of the overall area of the search space. As FOV size increases with all else being constant, targets are naturally found faster and so the average slope of the CDF also increases. Figure 5 demonstrates this relationship.

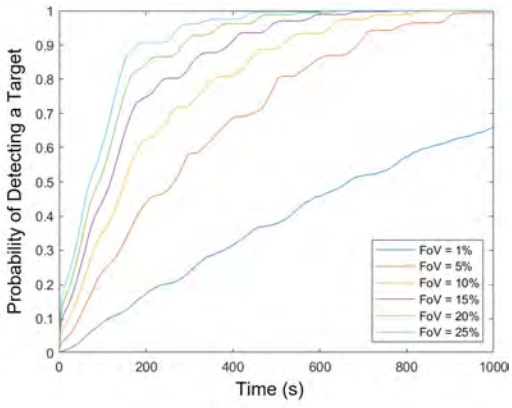

Figure 5: Relationship between FOV size and search pattern performance.

This research compares the Lissajous pattern with traditional patterns using a 1% FOV. Commercial drones on the market today have FOV angles ranging from less than 70° up to 180° or higher, and the Federal Aviation Administration limits drone altitude to 400 feet (Federal Aviation Administration 2023). Therefore, assuming a search agent with a 90° FOV angle flying at 400 feet, the camera could capture

approximately 0.23 square miles in its FOV. If modeling this scenario with a 1% FOV size, the simulation's total search space would be 23 square miles. Such a search scenario is demonstrated in Figure 6 over lower Manhattan Island. This qualitatively shows that a 1% FOV is reasonable for a large-scale mission searching for a sizeable target, but of course the simulation framework can easily be modified to meet any scenario-specific constraints. Because it was found that larger FOV sizes in fact favored the performance of Lissajous patterns, the 1% choice is both conservative and realistic.

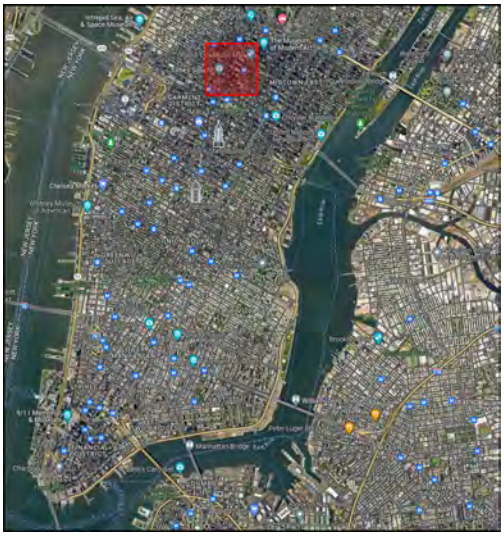

Figure 6: Real-world demonstration of a realistic 1% FOV search scenario over Manhattan.

2.6.3 Certainty Threshold

The certainty threshold is the level of confidence in finding a target which is satisfactory enough to designate a search mission as being complete. This parameter, which determines the upper bound in the expected value calculation, affects several aspects of the simulation. For example, the y-axis of Figure 4 which bears on the optimality of a Lissajous frequency ratio depends on the certainty threshold. If the desire is 100% certainty of finding a target without care for expediency, then the traditional patterns will inevitably be ideal. The benefit of the Lissajous curve is a trade-off in certainty for speed. However, this trade-off must still reflect an appropriate level of risk. With anything less than an 80% chance of locating the target, one may deem the approach too uncertain of success. On the other hand, high certainty thresholds de-value time, potentially increasing the risk associated with delayed target detection.

An externally supported justification for a reasonable certainty threshold is the "85% Rule for Optimal Learning" which presents 85% as the optimal training accuracy for artificial neural networks (Wilson et al. 2019). While the work presented here is not a machine learning algorithm, it is data-driven research looking to determine an acceptable error rate. Additionally, the United States Coast Guard had an approximately 87% success rate in 2017 SAR missions (4,188 lives saved versus 618 lives lost), which further justifies this ballpark as a realistic standard (Bureau of Transportation Statistics 2017). While the certainty threshold should reflect the modelled scenario, this research uses 85% as the certainty threshold metric for comparing search patterns.

2.6.4 Time Constant

The time constant parameter τ of Equation (2) models the quality of the detector by scaling how quickly the probability of detection increases over time as the agent traverses the search space. A small time constant yields a high probability of detecting a target inside of the agent's FOV quickly, whereas with larger time

constants, a target must be inside the FOV for a much longer time to yield such a high probability. Since the trajectories of a Lissajous path overlap and repeat, the certainty of locating a target will approach 100% given enough time. However, a single pass with the traditional patterns is not the same. Under the perfect detection assumption, those patterns are guaranteed to reach 100% certainty, but with probabilistic detection and a scaling parameter, the traditional patterns reach a maximum probability less than 1 as seen in Figure 9 in the Results.

Referencing back to the justifications for certainty threshold, this research aims to compare the Lissajous path to traditional patterns that are guaranteed to reach 85% certainty of target location in a single pass through the search space. As such, the results compare patterns using a time constant $\tau = 4$, which yields this desired "level-off" probability for the traditional search paths.

2.6.5 Target Distribution

The distribution of targets in a search space substantially influences the results of the Monte Carlo simulations and reflects the scenario that a given simulation is modeling. A uniform target distribution (Figure 7, left) produces targets located at any position in the search space with equal probability. A Gaussian target distribution (Figure 7, center) produces targets with a higher concentration in the center of the search space. A Reciprocal Gaussian target distribution (Figure 7, right) produces targets with a higher concentration along the perimeter of the search space.

Figure 7: Target Distributions: Uniform (left), Gaussian (center), Reciprocal Gaussian (right).

The simulations compare search patterns across these target distributions to observe the benefits of each pattern in different scenarios. The Uniform scenario can be considered the most general case, as a uniform distribution maximizes the information entropy about a target and best models the scenario where no prior information is known. The Gaussian distribution is used to broadly model a SAR scenario in which the last known location of the target is the center of the search space and the target will not move far since it wishes to be found. In contrast, the Reciprocal Gaussian distribution models a targeting scenario where an adversarial target that wishes not to be found is fleeing the search space. The Gaussian scenario naturally lends itself to the expanding spiral search pattern, but the hypothesis is that the Lissajous pattern will be particularly effective in locating evasive targets modeled with the Reciprocal Gaussian.

3 RESULTS AND DISCUSSION

To compare search pattern performance, the expanding spiral, horizontal sweep, and Lissajous patterns are evaluated against the three scenarios in Sec. 2.6.5. The FOV size, certainty threshold, and time constant are standardized among the scenarios for the provided justifications, with FOV$= 1\%$, Threshold$= 85\%$, and $\tau = 4$. A Uniform target distribution defines the general case (scenario 1), where the search patterns can be holistically evaluated without assuming any prior target knowledge. A Gaussian target distribution characterizes a simulated Search and Rescue mission (scenario 2) with the targets concentrated at the center of the search space. A Reciprocal Gaussian target distribution simulates a targeting mission (scenario 3) with the agent searching for an evasive target fleeing the search space. A Lissajous pattern is chosen for each scenario by optimizing its frequency ratio through direct search, and the chosen pattern is then compared to the traditional search patterns based on the evaluation metric described in Sec. 2.5. Table

1 summarizes the simulation parameters for each of the tested scenarios. Figure 8 shows the Lissajous patterns with optimal frequency ratios associated with each search scenario.

Table 1: Summary of simulation parameters for each scenario.

Scenario	Target Distribution	Optimal Frequency Ratio	FOV Size	Certainty Threshold	Time Constant
General Case	Uniform	0.8660	1%	85%	4
Search and Rescue	Gaussian	0.9531	1%	85%	4
Targeting	Reciprocal Gaussian	0.7789	1%	85%	4

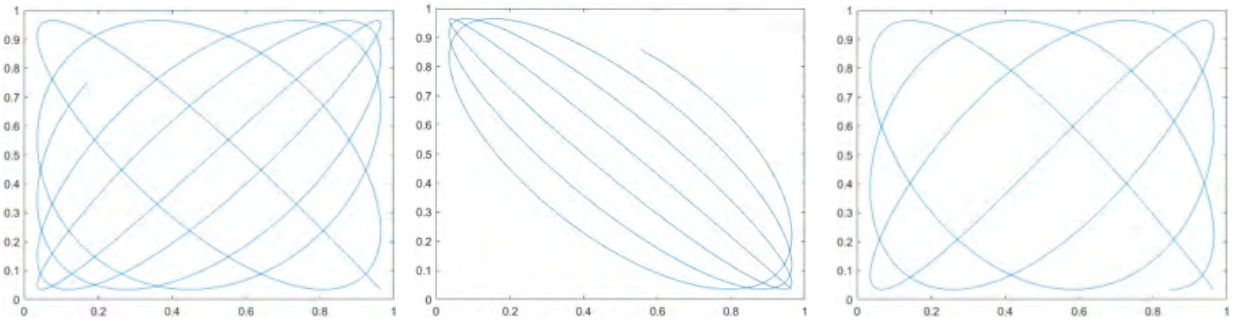

(a) General Case (b) Search and Rescue (c) Targeting

Figure 8: Optimal Lissajous patterns for each search scenario.

The three CDFs per scenario corresponding to the three search patterns are generated for visual comparison in Figure 9, and the expected values of each CDF are summarized in Table 2.

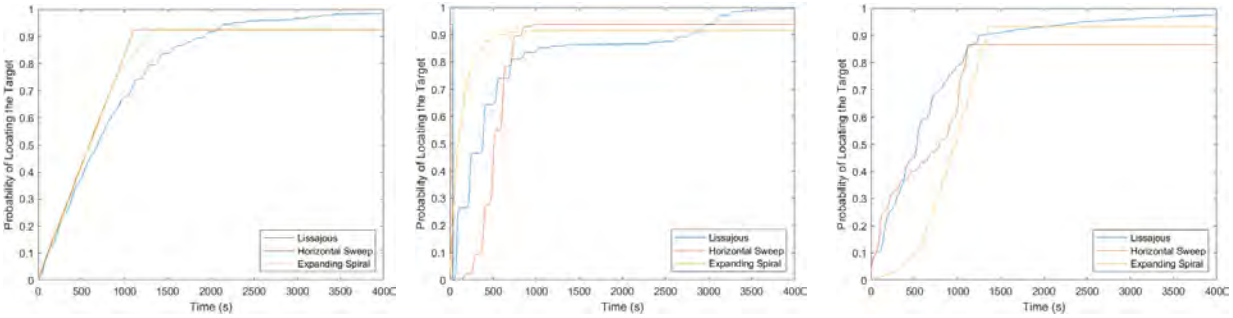

(a) General Case (b) Search and Rescue (c) Targeting

Figure 9: Cumulative Density Functions for each search pattern and scenario.

Table 2: Summary performance data for each search pattern by scenario.

	Expected Value from the CDF (seconds)		
Scenario	Expanding Spiral	Horizontal Sweep	Lissajous Pattern
General Case	609.78	**580.46**	756.33
Search and Rescue	**140.51**	528.68	426.61
Targeting	919.57	639.49	**557.62**

Figure 9a shows that traditional search patterns outperform the Lissajous in the general case. Both the expanding spiral and horizontal sweep maintain very similar performance for the duration of the simulation

until around 750 seconds when the expanding spiral begins its last pass around the search space. Because the agent's FOV overlaps the edge of the search space in this last pass, it accumulates probability at a decreased rate. The Lissajous pattern maintains similar performance to the traditional patterns for 500 seconds, but then its probability accumulation rate decreases steadily. While under-performing in comparison with the traditional patterns, the Lissajous still performs well for the uniform target distribution scenario. In fact, for FOVs greater than 1%, the Lissajous pattern was found to outperform the traditional patterns.

Unsurprisingly, the search and rescue scenario depicted in Figure 9b shows that the expanding spiral significantly outperforms both the horizontal sweep and the Lissajous pattern. A spiraling pattern is naturally tailored to search scenarios with a high target probability in the center of the search space with decreasing probability outward. However, the Lissajous pattern does beat out the horizontal sweep against a Gaussian target distribution with an expected value over 100 seconds faster. While the expanding spiral may be the ideal flight pattern for certain search and rescue missions, the Lissajous pattern is still a better search method than the horizontal sweep.

Figure 9c shows that the Lissajous pattern significantly outperforms the traditional search patterns in the targeting scenario. The expanding spiral performs quite poorly until $500-1,000$ seconds when it makes its final pass around the perimeter of the search space. The horizontal sweep's first trajectory traces the outside bottom perimeter of the search space, and as such, it performs similarly to the Lissajous pattern for the first 250 seconds. However, it begins to under-perform as it passes through the middle of the search space. The Lissajous pattern maintains strong performance for the full duration of the simulation when tested against a Reciprocal Gaussian target distribution.

4 CONCLUSION

The results primarily show that no flight path can be crowned the "standard" for all unmanned aerial search missions. Rather, every unique scenario calls for a search path best fit to the parameters of the situation. While not ideal for every scenario, the Lissajous pattern is in fact reasonable and even competitive for some search missions. Any situation with a concentrated probability at a particular location naturally lends itself to the expanding spiral pattern, and traditional patterns may be better suited for general search missions with unknown target behavior. However, these findings suggest that an optimized Lissajous pattern may be an effective flight path for evasive targets or in situations with concentrated probability around the perimeter of the search space.

Future work should expand on this research by implementing dynamic targets that can individually move in the simulation, rather than simulating target behavior with only a constant distribution. Additionally, next steps are to investigate ways of analytically optimizing the frequency ratio rather than relying on computationally expensive brute-force methods. Notwithstanding the improvements that future work could bring, this research further demonstrates the utility of the Lissajous pattern in certain search contexts.

REFERENCES

Ayers, J. R., and A. Wahlman. 2021. "A Concept for Next-Generation Combat Search and Rescue". *Air Space Power Journal* 35(2):68–76.

Blankenship, R., J. Bluman, and J. J. Steckenrider. 2021. "An Investigation of Search Algorithms for Aerial Reconnaissance of an Area Target". In *Proceedings of the Annual General Donald R. Keith Memorial Conference*, April 28th, 72–78.

Blankenship, R., J. Bluman, and J. J. Steckenrider. 2022. "Lissajous Patterns for Autonomous Chemical Agent Detection". Department of Mathematical Sciences, United States Military Academy, West Point, New York.

Bureau of Transportation Statistics. 2018. "U.S Coast Guard Search and Rescue Statistics, Fiscal Year". https://www.bts.gov/content/us-coast-guard-search-and-rescue-statistics-fiscal-year.

Dutta, G., and P. Goswami. 2020. "Application of Drones in Agriculture: A Review". *International Journal of Chemical Studies* 8:181–187.

IMO 2016. *International Aeronautical and Maritime Search and Rescue Manual*. London, UK and Montreal, CA: International Maritime Organization and International Civil Aviation Organization.

Federal Aviation Administration. 2023. "Recreational Flyers & Community-Based Organizations". https://www.faa.gov/uas/recreational_flyers#:-:text=Fly%20at%20below%20400,the%20UAS%20Facility%20Maps%20webpage.

Feller, W. 1971. *An Introduction to Probability Theory and Its Applications. Volume II*. 2nd ed. New York-London-Sydney: John Wiley & Sons, Inc.

Mishra, B., D. Garg, P. Narang, and V. Mishra. 2020. "Drone-Surveillance for Search and Rescue in Natural Disaster". *Computer Communications* 156:1–10.

Niedzielski, T. 2018. "Applications of Unmanned Aerial Vehicles in Geosciences: Introduction". *Pure and Applied Geophysics* 175:3141–3144.

Paucar, C., L. Morales, K. Pinto, M. Sanchez, R. Rodriguez et al. 2018. "Use of Drones for Surveillance and Reconnaissance of Military Areas". In *Proceedings of the 2018 International Multidisciplinary Conference of Research Applied to Defense and Security*, April 18th-20th, Salinas, Ecuador, edited by A. Rocha and T. Guarda, 119–132.

Steckenrider, J. J., S. Leamy, and T. Furukawa. 2020. "Cooperative Aerial Search and Localization Using Lissajous Patterns". In *2020 IEEE International Symposium on Safety, Security, and Rescue Robotics, SSRR 2020*, 233–240. Piscataway, New Jersey: Institute of Electrical and Electronics Engineers Inc.

Stone, L. 1975. *Theory of Optimal Search*. Elsevier.

United States Coast Guard Aviation History. 2008. "2008-Coast Guard UAS (UAV) Program Office Established". https://cgaviationhistory.org/2008-coast-guard-uas-uav-program-offic-established/.

Wilson, R., A. Shenhav, M. Straccia, and J. Cohen. 2019. "The Eighty Five Percent Rule for Optimal Learning". *Nature Communications* 10(4646):1–9.

AUTHOR BIOGRAPHIES

MITCHELL J. MILLER is an undergraduate student in the Department of Mathematical Sciences at the United States Military Academy studying applied statistics and data science. His primary research interest is in the area of predictive analytics and machine learning, but he also conducts simulation based research regarding automated drone search. His email address is mitchellmiller@westpoint.com.

VICTOR E. TRUJILLO II received his B.S. in Operations Research from the United States Military Academy, his M.S. in Mathematics and Statistics from Georgetown University, and his Ph.D. in Applied Science from William & Mary. He is an assistant professor in the Department of Mathematical Sciences at West Point, and his research and teaching interests include machine learning, high energy laser propagation, edge computing, and military applications. His email address is victor.trujillo@westpoint.edu.

JAMES E. BLUMAN received his B.S. in Mechanical Engineering from the United States Military Academy, his M.S. in Aerospace Engineering from Penn State, and his Ph.D. in Mechanical Engineering from the University of Alabama in Huntsville. He is an associate professor in the Department of Mathematical Sciences at West Point, and his research and teaching interests include robotics and small autonomous vehicles, flapping wing micro air vehicles, and nonlinear control theory. His email address is james.bluman@westpoint.edu.

J. JOSIAH STECKENRIDER received his B.S. in Engineering Physics from Taylor University and his M.S. and Ph.D. in Mechanical Engineering from Virginia Tech. He is an assistant professor in the Civil and Mechanical Engineering Department at West Point, and his research and teaching interests include estimation, robotics, dynamics, and controls. His email address is john.steckenrider@westpoint.edu.